CI

e-med
www.e-med.org.uk

ORIGINAL ARTICLE

Staging of neuroendocrine tumours: comparison of [68Ga]DOTATOC multiphase PET/CT and whole-body MRI

C. Schraml, N. F. Schwenzer, O. Sperling, P. Aschoff, M. P. Lichy, M. Müller, C. Brendle,
M. K. Werner, C. D. Claussen, C. Pfannenberg

University Department of Radiology, University Hospital of Tübingen, Hoppe-Seyler-Strasse 3, Tübingen 72076, Germany

Corresponding address: Dr Christina Schraml, MD, University Department of Radiology, University Hospital of Tübingen, Hoppe-Seyler-Strasse 3, Tübingen 72076, Germany.
Email: `christina.schraml@med.uni-tuebingen.de;`
`christina.b.schraml@googlemail.com`

Abstract

Purpose: In patients with a neuroendocrine tumour (NET), the extent of disease strongly influences the outcome and multidisciplinary therapeutic management. Thus, systematic analysis of the diagnostic performance of the existing staging modalities is necessary. The aim of this study was to compare the diagnostic performance of 2 whole-body imaging modalities, [68Ga]DOTATOC positron emission tomography (PET)/computed tomography (CT) and magnetic resonance imaging (MRI) in patients with NET with regard to possible impact on treatment decisions. **Materials and methods**: [68Ga]DOTATOC-PET/CT and whole-body magnetic resonance imaging (wbMRI) were performed on 51 patients (25 females, 26 males, mean age 57 years) with histologically proven NET and suspicion of metastatic spread within a mean interval of 2.4 days (range 0–28 days). PET/CT was performed after intravenous administration of 150 MBq [68Ga]DOTATOC. The CT protocol comprised multiphase contrast-enhanced imaging. The MRI protocol consisted of standard sequences before and after intravenous contrast administration at 1.5 T. Each modality (PET, CT, PET/CT, wbMRI) was evaluated independently by 2 experienced readers. Consensus decision based on correlation of all imaging data, histologic and surgical findings and clinical follow-up was established as the standard of reference. Lesion-based and patient-based analysis was performed. Detection rates and accuracy were compared using the McNemar test. P values <0.05 were considered significant. The impact of whole-body imaging on the treatment decision was evaluated by the interdisciplinary tumour board of our institution. **Results**: 593 metastatic lesions were detected in 41 of 51 (80%) patients with NET (lung 54, liver 266, bone 131, lymph node 99, other 43). One hundred and twenty PET-negative lesions were detected by CT or MRI. Of all 593 lesions detected, PET identified 381 (64%) true-positive lesions, CT 482 (81%), PET/CT 545 (92%) and wbMRI 540 (91%). Comparison of lesion-based detection rates between PET/CT and wbMRI revealed significantly higher sensitivity of PET/CT for metastatic lymph nodes (100% vs 73%; $P<0.0001$) and pulmonary lesions (100% vs 87%; $P=0.0233$), whereas wbMRI had significantly higher detection rates for liver (99% vs 92%; $P<0.0001$) and bone lesions (96% vs 82%; $P<0.0001$). Of all 593 lesions, 22 were found only in PET, 11 only in CT and 47 only in wbMRI. The patient-based overall assessment of the metastatic status of the patient showed comparable sensitivity of PET/CT and MRI with slightly higher accuracy of PET/CT. Patient-based analysis of metastatic organ involvement revealed significantly higher accuracy of PET/CT for bone and lymph node metastases (100% vs 88%; $P=0.0412$ and 98% vs 78%; $P=0.0044$) and for the overall comparison (99% vs 89%; $P<0.0001$). The imaging results influenced the treatment decision in 30 patients (59%) with comparable information from PET/CT and wbMRI in 30 patients, additional relevant information from PET/CT in 16 patients and from wbMRI in 7 patients. **Conclusion**: PET/CT and wbMRI showed comparable overall lesion-based detection rates for metastatic involvement in NET but significantly differed in organ-based detection rates with superiority of PET/CT for lymph node and pulmonary lesions and of wbMRI for liver and bone metastases. Patient-based analysis revealed superiority of PET/CT for NET staging. Individual treatment strategies benefit from complementary information from PET/CT and MRI.

Introduction

Neuroendocrine tumours (NETs) consist of a heterogeneous group of neoplasms with different biological behaviour and clinical presentation[11]. NETs originate from neuroendocrine cells most commonly from the gastroenteropancreatic tract or the bronchopulmonary system[2]. The annual incidence of NETs is 2.5–5 per 100,000 with a significant increase over the last decades[1,3]. This increase most probably reflects the growing clinical awareness of this entity and the continuous improvement in diagnostics[4]. The NET tumour group has great diversity regarding the primary tumour site, histopathology, proliferation markers, degree of invasiveness and production of biologically active substances[4,5]. In the new pathologic classification of NET proposed by the World Health Organization (WHO) in 2010, all NETs are supposed to be potentially malignant. According to the WHO classification, all well-differentiated neoplasms regardless of whether they behave benignly or develop metastases, are called neuroendocrine tumours and graded G1 or G2. All poorly differentiated neoplasms are termed neuroendocrine carcinomas and graded G3[6]. Depending on the histologic tumour grade, 20–50% of patients with NET have synchronous regional or distant metastasis at the time of diagnosis[3]. At present, surgical removal represents the only curative treatment option for NETs and is recommended if complete resection seems achievable based on cross-sectional imaging[3]. Other treatment options comprise palliative surgical debulking and tumour embolization, systemic treatment (somatostatin analogues, interferon-α, chemotherapy or anti-angiogenetic drugs) and peptide receptor radionuclide therapy[5,7]. Given the complexity of tumour behaviour and treatment strategy, patients with NET require multidisciplinary care for the most favourable management[1].

Most NET cells express somatostatin receptors (SSR), which can be targeted by labelled somatostatin analogues (SSAs). This approach can be used both for diagnostic and therapeutic applications[8]. Recently, combined positron emission tomography (PET)/computed tomography (CT) with 68Ga-labelled SSA as radiotracer has proved to be highly effective in diagnostic imaging of NETs[9–13]. Besides PET/CT, whole-body magnetic resonance imaging (wbMRI) represents another valuable modality in the diagnostic work-up of oncologic patients[14–17] and has also proved valuable in the detection of NET metastases[18–20]. Nevertheless, in clinical routine, the optimal whole-body imaging modality for NET assessment is still under debate.

The aim of this study was to compare the diagnostic performance of [68Ga]DOTATOC PET/CT and wbMRI regarding lesion detection and staging with a view to potential influence on clinical management of patients with NET.

Materials and methods

Patients

From 2006 to 2009, 51 consecutive patients (25 females, 26 males; mean age 57 years) with histologically proven NET and suspicion of metastatic spread were referred to our department for staging by PET/CT and wbMRI. After being informed about the study procedures and signing informed consent approved by the ethics committee, PET/CT and wbMRI were performed on each patient within an interval of less than 30 days (mean 2.4 days, median 1 day; range 0–28 days).

Primary tumour sites were the gastroenteropancreatic system ($n = 32$), thyroid ($n = 2$), bronchopulmonary system ($n = 2$), thymus ($n = 2$), cervix ($n = 2$), parotid gland ($n = 1$), cranium ($n = 1$), adrenal gland ($n = 1$) and unknown ($n = 8$). In 20 patients the tumour was well differentiated (G1), in 7 patients moderately differentiated, in 20 patients poorly differentiated (G3) and in 4 patients tumour grading was not known.

wbMRI

All MRI examinations were performed on a whole-body 1.5-T system with multiple phased-array surface coils and receiver channels using an integrated parallel acquisition technique (Avanto, Siemens Healthcare, Erlangen, Germany). MR images in coronal (wb) and axial (head, thorax, abdomen, pelvis) slice orientation were obtained in 5 subsequent table positions. The examination protocol comprised the following sequences:

- whole-body: short tau inversion recovery (STIR) turbo spin echo (TSE) (coronal)
- thorax: STIR TSE (coronal) and T1 volume interpolated breathhold examination (VIBE) 3D (axial)
- abdomen: navigator respiratory-triggered T2 TSE fatsat (axial), T1 fast low angle shot MRI (FLASH) 2D fatsat (axial)
- pelvis: T2 STIR TSE (axial)
- dynamic series covering the abdomen: T1 VIBE 3D fatsat (coronal)
- post contrast: whole-body T1 FLASH 2D fatsat (axial)

Contrast-enhanced series were performed after intravenous administration of 0.2 ml of gadopentetate dimeglumine (Magnevist, Schering, Berlin, Germany) per kilogram of body weight. Total examination time was about 1 h. The sequence protocol has been described in detail in a previous study[16].

PET/CT imaging

PET/CT was performed using the Hi-Rez Biograph 16 (Siemens Medical Solutions, Knoxville, TN), which consists of a high-resolution 3D lutetium oxyorthosilicate (LSO) PET and a 16-row multi-detector CT. All patients were asked to drink 1000 ml of mannitol 2% as a negative oral contrast agent before the PET/CT examination to distend the bowel. To reduce intestinal motility, a 20–40 mg dose of scopolamine butylbromide (Buscopan; Boehringer Ingelheim, Ingelheim, Germany) was injected intravenously before the start of the image acquisition.

PET protocol

PET imaging started 30 min after intravenous administration of 150 MBq of [^{68}Ga]DOTATOC. Emission data were recorded from the base of the skull to the upper thigh with an acquisition time of 3 min per bed position. The attenuation-corrected PET data were iteratively reconstructed using an attenuation-weighted ordered-subset maximization expectation (OSEM) algorithm (4 iterations, 8 subsets, 128×128 matrix, gaussian post-filtering of 5 mm, voxel size $5.3 \times 5.3 \times 5$ mm^3) on a Syngo^{TM} workstation (Version VD20K; Siemens Medical Solutions) and co-registered with the CT data using the commercially available software (TrueD, Siemens, Erlangen, Germany).

CT protocol

For attenuation correction of PET data, a low-dose CT scan (30 mAs) was acquired before the contrast-enhanced multiphase CT protocol. Afterwards, a contrast-enhanced CT scan was performed. To improve diagnostic significance, a multiphase CT protocol consisting of a bolus-triggered arterial phase scan (head/neck-thorax-abdomen) and a portovenous phase scan (abdomen-pelvis-upper thigh) was performed with administration of 120 ml of iodinated contrast agent (Ultravist 370; Bayer Schering Pharma, Berlin, Germany) with an injection flow rate of 3 ml/s. To prevent contrast-induced artefacts, the injection protocol was optimized with a 40-ml saline chaser following contrast application.

The CT scan parameters were as follows: tube voltage 120 kV, 120–160 mAs, rotation time 0.5 s, collimation 0.75 mm (thorax) and 1.5 mm (abdomen). The reconstructed slice thickness/increment was 5/5 mm (axial) and 3/2 mm (coronal).

Image analysis

Image analysis was performed separately for each modality (PET, CT and MRI) and for the combined PET/CT by 2 specialists in nuclear medicine and 2 experienced radiologists, respectively. For each site (lung, liver, bone, lymph node, other), the number of lesions detected was noted. If more than 10 lesions were present in one site, 11 lesions were considered for the final evaluation. The readers were blinded to the results of any other imaging study and previous tests. The consensus decision was made in a second reading session 6–8 weeks after the first session, lesion by lesion, by all readers.

In PET images, focal uptake exceeding normal regional tracer accumulation was classified as a malignant lesion. Uptake without a morphologically suspicious imaging correlate in regions with known physiologic uptake (e.g. pancreas, liver, spleen, pituitary, thyroid, kidneys, adrenal glands, salivary glands, bowel wall, prostate, breast) was not classified as metastatic[21,22]. If focal uptake was seen in the uncinate process without a morphological correlate on CT, this was attributed to physiologic uptake most probably due to the presence of SSR on islet cells[23]. If symmetric uptake was seen in the hilar nodes, this was attributed to an inflammatory or granulomatous condition and not judged to be metastatic disease. On CT and MR images, the assessment of a malignant lesion was based on standard reading criteria established in clinical practice by taking into account morphologic features and enhancement characteristics. A lesion was called SSR+ when showing DOTATOC uptake on PET. A lesion was defined as SSR− when showing no uptake on PET.

Standard of reference

As a histopathology-based gold standard was not realizable for every lesion detected, the consensus decision (based on correlation of all available image data, histologic and surgical findings where available and clinical follow-up) was established as a surrogate standard of reference. Radiologic follow-up data comprised a period of at least 12 months.

Data evaluation

Based on the standard of reference, lesion- and patient-based evaluation was performed. For the lesion-based analysis, all lesions were categorized as true-positive, true-negative or false-positive and modality-based detection rates with their 95% confidence intervals (CI) were calculated. In the patient-based analysis, patients were classified as being positive (with metastases regardless of the number of metastases per organ site) or negative (without metastases) for defined organ categories. In this evaluation, the number of true-negatives was known and sensitivity, specificity and accuracy with their 95% CI were calculated.

Influence of imaging on the treatment decision

The study took place in a clinical context. Therefore, most patients were referred for evaluation of further treatment options after they had already undergone surgery and other treatment elsewhere. Pretest management

plans based on conventional imaging results were categorized in the following groups: observation, local therapy (resection/ablation) and ongoing systemic therapy. Resection was classified as curative treatment. All other therapies were categorized as being palliative.

After PET/CT and MRI scans of the patients, the therapeutic strategy was discussed and decided by the interdisciplinary tumour board formed by members from the departments of oncology, pathology, radio-oncology, surgery, radiology and nuclear medicine. Board members considered the results of both imaging studies (PET/CT and MRI). Treatment decisions were taken according to the European Neuroendocrine Tumour Society (ENETS) guidelines[24,25]. The previous treatment plan was compared with the treatment decision of the interdisciplinary tumour board. To analyze the impact of each whole-body modality on therapeutic management, the modality that provided the most relevant information for treatment decision was noted. Thus, the following conditions were defined:

- comparable information obtained from both modalities (PET/CT and MRI)
- additional relevant information from PET/CT
- additional relevant information from MRI

Statistical analysis

Comparison of lesion-based detection rates and organ-based accuracy of PET/CT and MRI was performed using the McNemar test for binary outcome data in dependent samples. A P value < 0.05 was considered statistically significant. All statistical analyses were performed using the statistical software package JMP (version 9.0, SAS Institute, Cary, NC). To consider the influence of SSR expression on the diagnostic performance of PET and PET/CT, a separate analysis was performed for SSR positive (SSR+) and SSR negative (SSR−) lesions.

Results

According to the standard of reference, metastatic lesions were found in 41 of 51 (80%) patients. In these 41 patients, a total of 593 NET metastases were evaluated. Metastatic lesions were located in the lung ($n = 54$), liver ($n = 266$), skeleton ($n = 131$), lymph nodes ($n = 99$) and other sites (e.g. soft tissue, bowel, mesentery) ($n = 43$). Table 1 summarizes the number of metastases per patient with respect to organ category. Median lesion number±standard deviation per patient was 9 ± 12, ranging from 0 to 41. Thirty-seven percent of patients had more than 10 liver metastases, 8% of patients had more than 10 lung metastases, 22% of patients had more than 10 bone metastases and 10% had more than 10 lymph node metastases.

Table 1 **Number of organ metastases per patient**

Number of metastases	Number of patients (%)			
	Liver	Lung	Bone	Lymph nodes
>10	19 (37)	4 (8)	11 (21)	5 (10)
5–10	6 (12)	0 (0)	0 (0)	2 (4)
1–5	4 (8)	4 (8)	6 (12)	16 (31)
0	22 (43)	43 (84)	34 (67)	28 (55)

The table summarizes the distribution of the number of organ metastases in the present study. The number in parentheses gives the percentage referred to all patients in the study ($n = 51$). Median lesion number ± standard deviation per patient was 9 ± 12 (range 0–41).

Lesion-based analysis

A detailed summary of site-based and overall analysis on a lesion basis is given in Table 2. Of all 593 detected lesions, PET identified 381 (64%) true-positive lesions, CT 482 (81%), PET/CT 545 (92%) and wbMRI 540 (91%). Overall detection rates of PET/CT and wbMRI were comparable (92% and 91%; $P = 0.07$). Site-based detection rates differed significantly with higher detection rates with PET/CT for metastatic lymph nodes (100% vs 73%; $P = 0.0001$) and pulmonary lesions (100% vs 87%; $P = 0.0233$), whereas wbMRI was superior in the detection of liver metastases (99% vs 92%; $P = 0.0001$) and bone lesions (96% vs 82%; $P = 0.0001$). Of all 593 lesions detected, 22 were found only on PET imaging, 11 were seen only on CT and 47 only on wbMRI. Modality-based analysis showed that 13 lesions were falsely rated as being metastatic on PET imaging, 43 lesions on CT and 53 on wbMRI, whereas only 7 lesions were false-positive on combined PET/CT imaging. Most of the false-positive lesions were attributable to lymph nodes as verified by follow-up studies.

In 5 patients (2 males, 3 females; mean age 53.6 years, range 18–75 years), 120 PET-negative lesions were detected by CT or MRI. The primary tumour site in these 5 patients was the pancreas ($n = 2$), thymus ($n = 1$), thyroid ($n = 1$) and unknown ($n = 1$). Two of the 5 patients had both PET-positive and PET-negative lesions. Separate analysis of PET-positive lesions (right part of Table 2) revealed a significantly higher overall detection rate of PET/CT in comparison with wbMRI (93% vs 90%; $P = 0.0003$).

Patient-based analysis

The results of the overall patient-based comparison of the 4 imaging modalities are summarized in Table 3. In this patient-based overall analysis, PET/CT and MRI showed comparable sensitivity (98%) for the assessment of the metastatic status of the patient, whereas PET/CT had slightly higher specificity and accuracy compared with MRI. Discrepancy between the PET/CT and MRI staging results occurred in 3 patients. In 1 patient, MRI was false-positive (liver), in 1 patient PET/CT was false-negative (bone) and in 1 patient, MRI was false-negative (lymph node).

Table 2 **Lesion-based comparison of [⁶⁸Ga]DOTATOC-PET/CT and wbMRI in 51 patients with NET**

Organ involvement	No. of lesions		Modality	All lesions (n = 593)						SSR+ lesions (n = 120)					
	All	SSR+		TP	FP	FN	Detection rate (%)	95% CI	P value: PET/CT vs MRI	TP	FP	FN	Detection rate (%)	95% CI	P value: PET/CT vs MRI
Lung	54	32	PET	4	1	50	7	2–18		4	1	28	13	4–29	0.0233
			CT	54	0	0	100	93–100		32	0	0	100	89–100	
			PET/CT	54	0	0	100	93–100	0.0233	32	0	0	100	89–100	
			MRI	47	1	7	87	75–95		25	1	7	78	60–91	
Liver	266	211	PET	169	0	97	64	57–69		169	0	42	80	74–85	<0.0001
			CT	226	3	40	85	80–89		171	3	40	81	75–86	
			PET/CT	245	0	21	92	88–95	<0.0001	190	0	21	90	85–94	
			MRI	264	11	2	99	97–99		209	11	2	99	97–100	
Bone	131	98	PET	90	0	41	69	60–77		90	0	8	92	85–96	0.2482
			CT	81	0	50	62	53–70		63	0	35	64	54–74	
			PET/CT	108	0	23	82	75–89	<0.0001	90	0	8	92	85–96	
			MRI	126	2	5	96	91–99		93	2	5	95	89–98	
Lymph nodes	99	97	PET	96	3	3	97	91–99		96	3	1	99	94–100	<0.0001
			CT	87	38	12	88	80–94		85	36	12	88	79–93	
			PET/CT	99	4	0	100	96–100	<0.0001	97	4	0	100	96–100	
			MRI	72	34	27	73	63–81		70	24	27	72	62–81	
Other organs	43	35	PET	22	5	21	51	36–67		22	5	13	63	45–79	0.2482
			CT	33	2	9	79	61–88		25	1	9	74	54–85	
			PET/CT	39	3	4	91	78–97	0.0133	31	2	4	89	73–97	
			MRI	31	5	12	72	56–85		28	5	7	80	63–92	
Total	593	473	PET	381	9	212	64	60–68		381	9	92	81	77–84	0.0003
			CT	481	43	111	81	78–84		376	40	96	80	76–83	
			PET/CT	545	7	48	92	89–94	0.0736	440	6	33	93	90–95	
			MRI	540	53	53	91	88–93		425	43	48	90	87–92	

Comparison of overall and site-based detection rates of [⁶⁸Ga]DOTATOC-PET/CT and wbMRI in 51 patients with NET. Data are shown separately for all lesions (left) and for PET-positive (SSR+) lesions (right). NET, neuroendocrine tumour; TP, true-positive; FP, false-positive; FN, false-negative; SSR+, PET-positive, indicating somatostatin receptor expression; CI, confidence interval.

Table 3 **Patient-based overall analysis regarding detection of metastases in patients with NET**

Modality	TP	TN	FP	FN	Sensitivity (%)	95% CI	Specificity (%)	95% CI	Accuracy (%)	95% CI
PET	36	9	1	5	88	74–96	90	56–100	88	76–96
CT	37	9	1	4	90	77–97	90	56–100	90	76–96
PET/CT	40	10	0	1	98	87–100	100	69–100	98	90–100
MRI	40	9	1	1	98	87–100	90	56–100	96	87–100

The table summarizes the patient-based overall analysis of each imaging modality for the detection of metastatic involvement. Patient's status was classified as true-positive/-negative and false-positive/-negative for the presence of metastases. Sensitivity, specificity and accuracy are given with the 95% confidence interval. TP, true-positive; FP, false-positive; FN, false-negative; TN, true-negative; CI, confidence interval.

In the separate organ-based analysis per patient, which is summarized in Table 4, the diagnostic accuracy of PET/CT was significantly higher in the site-based evaluation for bone and lymph node metastases (100% vs 88%; $P = 0.0412$ and 98% vs 78%; $P = 0.0044$) and in the overall comparison (99% vs 89%; $P = 0.0001$). No significant difference was found between PET/CT and wbMRI in the other organ categories.

Impact on treatment management

In 30 of 51 patients (59%), the results of whole-body imaging led to a change in therapeutic strategy (Table 5). Curative treatment was the aim in 4 patients, whereas the primary treatment strategy changed from curative to palliative in 9 patients. In 12 patients, the palliative strategy was modified (alteration of systemic chemotherapeutics, induction or abandonment of radionuclide therapy). PET/CT and wbMRI provided comparable information for the treatment decision in 30 of 51 patients (59%) (Table 4); additional relevant information was obtained by PET/CT in 16 patients (31%) and by MRI in 7 patients (14%). In 2 patients, relevant information for treatment planning was obtained by PET/CT and MRI. PET/CT mainly provided relevant information concerning SSR expression and DOTATOC uptake, respectively, which was essential for the decision on the use of peptide receptor radionuclide therapy (PRRT). In contrast, additional MRI information mainly comprised the detailed evaluation of the hepatic infiltration pattern.

Discussion

Whole-body imaging is a substantial component of modern management in clinical oncology. Diagnosis,

Table 4 **Patient-based analysis of the diagnostic performance of PET, CT, PET/CT and MRI for metastatic organ involvement in patients with NET**

Organ involvement (no. of patients)	Modality	TP	FP	FN	TN	Sensitivity (%)	95% CI	Specificity (%)	95% CI	Accuracy (%)	95% CI	P value: accuracy of PET/CT vs MRI
Lung ($n=8$)	PET	3	1	5	42	38	8–76	98	88–100	88	76–96	0.2482
	CT	8	0	0	43	100	63–100	100	92–100	100	93–100	
	PET/CT	8	0	0	43	100	63–100	100	92–100	100	93–100	
	MRI	6	1	2	42	75	34–97	98	88–100	94	84–99	
Liver ($n=29$)	PET	24	0	5	22	83	64–94	100	85–100	90	79–97	0.4795
	CT	26	1	3	21	90	73–98	95	77–100	92	81–98	
	PET/CT	29	0	0	22	100	88–100	100	85–100	100	93–100	
	MRI	28	1	1	21	97	82–100	95	77–100	96	87–100	
Bone ($n=17$)	PET	14	0	3	34	82	57–96	100	90–100	94	84–99	0.0412
	CT	13	0	4	34	76	50–93	100	90–100	92	81–98	
	PET/CT	17	0	0	34	100	80–100	100	90–100	100	93–100	
	MRI	13	2	4	32	76	50–93	94	80–99	88	76–96	
Lymph nodes ($n=23$)	PET	20	1	3	27	87	66–97	96	82–100	92	81–98	0.0044
	CT	20	6	3	22	87	66–97	79	59–92	82	69–92	
	PET/CT	23	1	0	27	100	85–100	96	82–100	98	90–100	
	MRI	16	4	7	24	70	47–87	86	67–96	78	65–89	
Other organs ($n=17$)	PET	13	2	4	32	76	50–93	94	80–99	88	76–96	0.0736
	CT	13	1	4	33	76	50–93	97	85–100	90	79–97	
	PET/CT	16	0	1	34	94	71–100	100	90–100	98	90–100	
	MRI	15	4	2	30	88	64–98	88	73–97	88	76–96	

The table summarizes the patient-based analysis of the diagnostic performance of each imaging modality with regard to metastatic organ involvement in the predefined categories. Positive here means that the organ had metastatic involvement regardless of the number of lesions. Sensitivity, specificity and accuracy are given with the 95% confidence interval. TP, true-positive; FP, false-positive; FN, false-negative; TN, true-negative; CI, confidence interval.

Table 5 **Influence of PET/CT and MRI imaging on treatment decisions in patients with NET**

	No. of patients	%
Treatment decision		
No change in treatment	21	41
Primary curative approach	4	8
Primary palliative approach	5	10
Change from curative to palliative approach	9	18
Change in palliative strategy	12	24
Which image modality provided relevant information for treatment decision?		
Comparable information on PET/CT and MRI	30	59
Additional information on PET/CT (PET component)	16	31
Additional information on MRI	7	14

tumour staging and therapy monitoring strategies increasingly depend on data from morphologic and functional molecular imaging modalities such as wbMRI and PET/CT. In the present study, these 2 important whole-body imaging modalities were compared in patients with NET. This comparison has been motivated by the clinical awareness that accurate staging has a strong impact on the guidance of multimodal treatment options for patients with NET[3,12].

In the lesion-based analysis, the overall detection rates of PET/CT and wbMRI were comparable, whereas clear site-based differences were found with superiority of [68Ga]DOTATOC-PET/CT for detection of lung and lymph node metastases and of wbMRI for bone and liver metastases. The differences observed underline the clinical relevance of both whole-body imaging modalities in the oncologic staging of patients with proven or suspected metastatic NET. Both PET/CT and wbMRI proved superior to CT and PET alone. The relatively high detection rate for hepatic metastases of CT alone (85%) is most probably attributable to the multiphase CT protocol. In the present study design from a clinical point of view, the lesion-based specificity of each modality could not be calculated as obviously benign lesions such as hepatic cysts were not documented.

In the patient-based analysis, PET/CT and wbMRI revealed comparable sensitivity and accuracy for the classification of the whether the patient had metastasis or not

(Table 3). When looking at the patient-based analysis regarding metastatic involvement of different organs, the diagnostic accuracy of PET/CT was significantly higher for bone and lymph node metastases. In contrast to the lesion-based analysis, the diagnostic accuracy of PET/CT and MRI were comparable for lung and liver metastases in the patient-based analysis. The discrepant results in the lesion- and patient-based analyses emphasize the influence of the evaluation scheme on the study results when comparing the diagnostic performance of imaging modalities in the staging of oncologic patients.

The patient-based analysis is most important for the initial work-up of patients with NET when the categorization has to be made on whether there are metastases present or not. However, once the patient's status is categorized as metastatic, the diagnostic work-up has to move a step further. Then, it is required to accurately assess the number and localization of metastases so that the best individual treatment plan for each patient can be defined. Once in this phase of the diagnostic work-up, a patient-based comparison might no longer suffice to find the best staging modality.

In general, the most important staging factor that influences the clinical management is resectability. Thus, in most cases, the presence or absence of organ metastases is crucial and this can mostly be described based on patient/organ status (metastatic or not) rather than on lesion counts. However, in selected cases with limited disease extent, the number and even the distribution pattern of lesions per organ are used to decide on resectability. In these cases, lesion-based comparison of imaging modalities is more important. Therefore, interpretation of the study results needs to be done with respect to the precise clinical question.

In our study, 5 of 41 patients (12%) had lesions that showed no [68Ga]DOTATOC uptake. This percentage is in accordance with the literature[26]. In these 5 patients, 120 SSR− lesions (more than 20% of all lesions evaluated) were found and contributed to the results, which may explain the relatively low detection rate for PET. Separate evaluation of SSR+ only patients revealed higher PET and PET/CT detection rates both in the site-based evaluation and in the overall analysis (Table 2). Moreover, in the separate evaluation of SSR+ lesions, significant differences between PET/CT and wbMRI were only found for liver and lymph node metastases with superiority of PET/CT for metastatic lymph node assessment and MRI for detection of liver metastases. However, the diagnostic performance derived from analysis of only SSR+ lesions does not reflect the situation in clinical routine, where the actual receptor status of each NET lesion is unknown. Moreover, SSR expression can vary by tumour cell type and over the time course of disease[27]. SSR expression may also be variable in different lesions in the same patient (Fig. 1). Histologic correlation of each lesion, however, is not feasible and not ethically justifiable, especially in cases of extended tumour burden, so that in clinical routine the receptor status of each lesion is not known at the time point of the PET/CT scan.
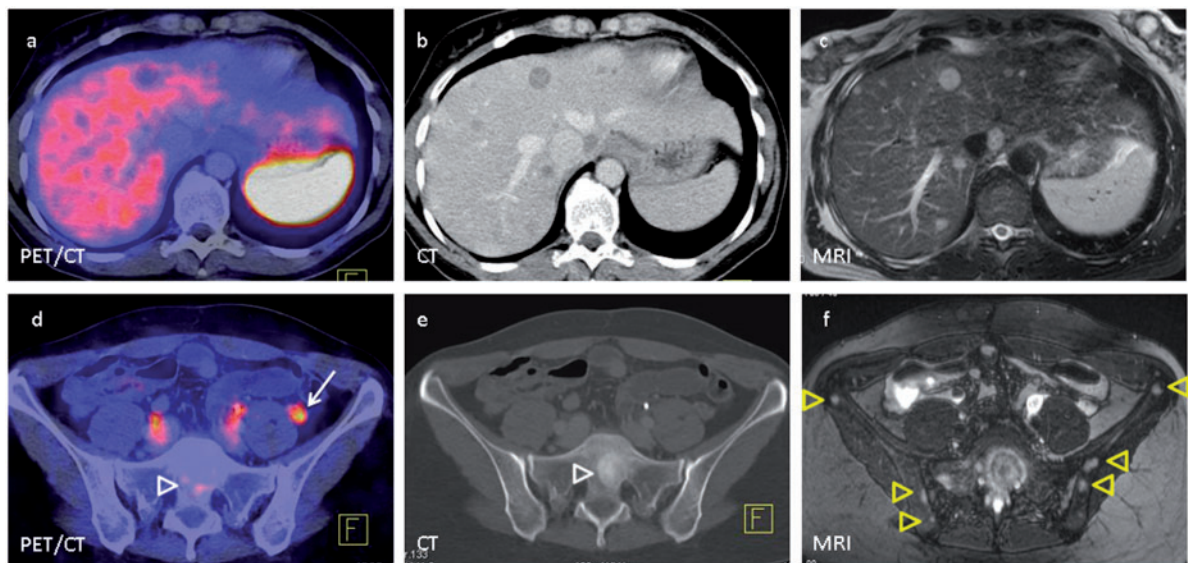
Figure 1 **A 37-year-old woman with metastatic NET, originating from the cervix uteri, with variable SSR expression of the metastatic lesions. Upper row (a–c): axial slices at the level of the liver; lower row (d–f): axial slices at the level of the pelvis. Multiple metastatic liver lesions on CT (b) and MRI (c) without any detectable [68Ga]DOTATOC uptake in PET (a). Marked [68Ga]DOTATOC uptake of a metastatic lesion situated ventral to the left m. psoas (white arrow, d) in the same patient. CT shows sclerotized bone metastases in the os sacrum (e, arrowhead) with only slight uptake (d, arrowhead). The MR image at the same level reveals multiple additional bone lesions (yellow arrowheads, f) not visible on PET or CT.**

Regarding the importance of imaging for clinical decision making, we agree with the results of Frilling et al.[12] who investigated the impact of whole-body [68Ga]DOTATOC-PET/CT on the multimodal management of NETs. Frilling et al.[12] found a change in the treatment regimen based on imaging information in more than every second patient, which is in accordance with our results. In our study, for most patients (59%), PET/CT and MRI provided comparable information for the treatment decision. PET/CT provided additional information in 31% of patients. This was mainly attributable to the evaluation of SSR expression as assessed by DOTATOC uptake in PET. This is in accordance with the literature[28]. When looking at the SSR– lesions only, CT was able to detect metastatic liver involvement in all of these PET-negative cases and thus compensated for the missing detectability in PET in the hybrid modality PET/CT. This may be attributed to the multiphase CT protocol, which facilitates the detection of hypervascularized NET lesions in the liver. In 6 patients, exact assessment of the metastatic liver infiltration pattern obtained by MRI significantly influenced the treatment decision. All these patients had a limited number of liver metastases (<10).

NETs have great variability in cellular differentiation, which makes the choice of tracer challenging. The 2 compounds most often used in functional imaging with radiolabelled somatostatin analogues are [68Ga]DOTATATE and [68Ga]DOTATOC. In the present study, [68Ga]DOTATOC was used. Poeppel et al.[29] found that [68Ga]DOTATOC and [68Ga]DOTATATE have a comparable diagnostic value for the detection of NET lesions. Therefore, the study results can be considered representative. It has been shown that fluorodeoxyglucose (FDG) is of limited value in well-differentiated NET due to the almost normal glucose turnover[30]. Poorly differentiated NETs, however, tend to show higher metabolic turnover and less expression of SSR. Kayani et al.[31] compared the radiolabelled somatostatin analogue [68Ga]DOTATATE with [18F]FDG in the diagnosis of NET. They found that DOTATATE-PET/CT was superior to FDG-PET/CT for imaging well-differentiated NET and that functional imaging with both DOTATATE and FDG could possibly provide a more comprehensive tumour assessment in intermediate- and high-grade NETs[31]. For the present study, a radiolabelled somatostatin analogue was chosen as the PET tracer because patients were referred to the PET/CT scan for staging and treatment evaluation. DOTATOC-PET allows the radionuclide uptake to be evaluated, which is linked to radiopeptide therapy efficacy[32]. Studies indicate that receptor status can be predicted by immunohistochemistry[33]. However, in a clinical setting it is impossible to obtain histologic correlation for each lesion. Therefore, information about the receptor status of all lesions and the intensity of somatostatin analogue uptake can only be obtained by SSR scintigraphy or PET. This is a major drawback of wbMRI in comparison with PET/CT, which might be neglected when merely looking at differences in detection rates.

The complementary role of MRI in NET assessment might be optimized by adding functional imaging sequences such as diffusion-weighted imaging (DWI) to the MR protocol. DWI has proven valuable in oncologic MRI both for tumour detection and characterization because it offers a high lesion-to-background contrast and provides information about tumour cellularity and cell membrane integrity[34]. In addition, dynamic contrast-enhanced MRI provides perfusion parameters, which, like DWI parameters, can be correlated with functional parameters such as receptor expression or metabolism as obtained by PET. These parameters are expected to be particularly helpful in evaluating individual treatment-induced changes in NETs. The recently introduced hybrid MR/PET systems[35] therefore may have considerable potential for the multiparametric assessment of NETs.

Our study is limited by the fact that histologic correlation could not be obtained for each lesion for technical and ethical reasons due to the advanced stage of metastatic dissemination in most of the patients included in our study. Thus, lesion classification was based on standard reading criteria as reported in the literature[36–38]. Moreover, the study was based on comparison of all NET metastases detected by PET/CT and wbMRI and defined by the reference standard. This implies that some NET metastases might have been missed by all modalities and clinical findings so that the actual true number of false-negative lesions is not known[13]. Therefore, the term detection rate instead of sensitivity was preferred in the lesion-based analysis. The results of our study should be interpreted with awareness that the number of metastases per organ influences the overall detection rates. Our patient collective had a relatively high number of liver metastases (266), so that the diagnostic performance of each imaging modality is strongly influenced by the sensitivity for liver metastases (Fig. 2). This influence might even be underestimated when looking at our results because the study design prescribed evaluation of a maximum number of 11 lesions per site. This number was chosen arbitrarily and might be considered relatively high. However, we wanted to make sure that a representative number of lesions could be evaluated.

The superiority of MRI for detecting hepatic lesions is mainly attributable to the excellent soft tissue contrast and the high spatial resolution of MRI compared with PET and CT. However, as the patients were consecutively enrolled in the study, the high prevalence of liver metastases in NETs most probably represents clinical reality.

Conclusion

PET/CT and wbMRI showed comparable overall lesion-based detection rates for metastatic involvement in NET
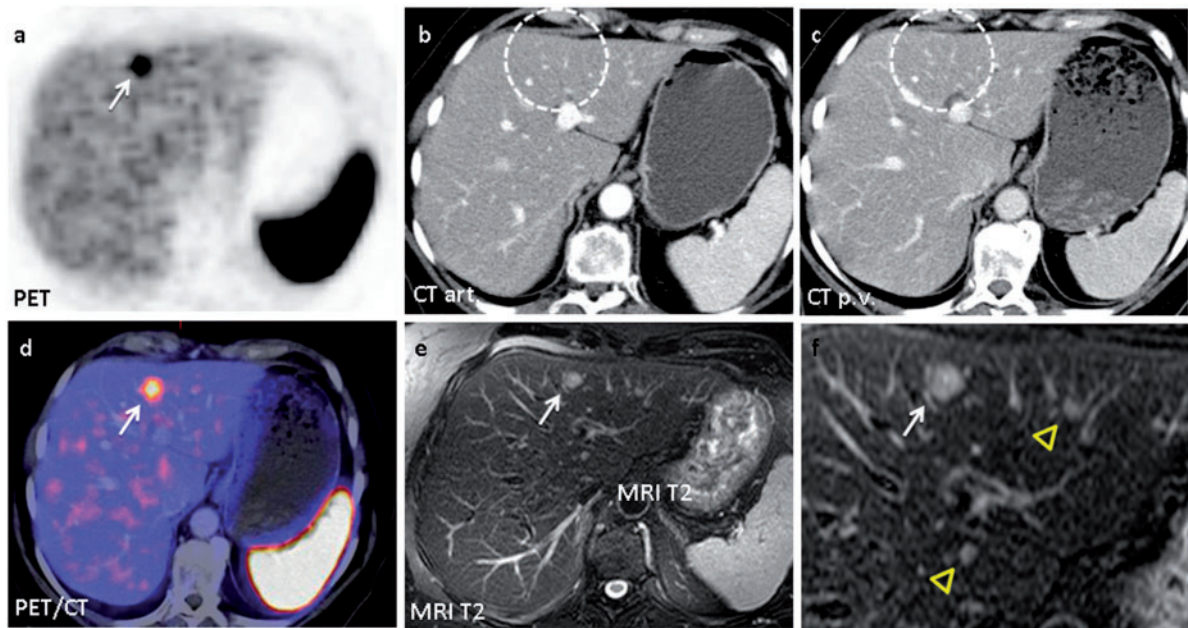
Figure 2 **A 61-year-old woman with hepatic metastases of NET originating from the ileum (ileal carcinoid). Axial slices at the level of the liver: (a) PET, (b) contrast-enhanced CT in the arterial phase, (c) contrast-enhanced CT in the portovenous phase, (d) fusion PET/CT, (e) MRI T2, (f) MRI T2 magnification view of (e). In the PET (a) and in the fused PET/CT image (d), a PET-positive metastatic lesion is seen in segment IV A of the liver (white arrow). In the contrast-enhanced CT images (b, c), the lesion is neither visible in the arterial (b) nor in the porto-venous (c) phase (dotted circle). In the T2-weighted MR images (e, f), the lesion is clearly depicted (e, f, white arrow). Furthermore, additional metastases can be seen in the same lobe (f, yellow arrowheads).**

but significantly differed in organ-based detection rates; PET/CT was superior for lymph node and pulmonary lesions and wbMRI was superior for liver and bone metastases. Patient-based analysis revealed superiority of PET/CT for NET staging. Individual treatment strategy benefits from complementary information from PET/CT and MRI. From a patient-based analysis point of view, PET/CT proved to be the most powerful staging tool providing therapy-relevant information, especially in patients with extended metastatic spread when PRRT is the aim. However, as NET treatment decisions are highly individualized and strongly depend on the presence and pattern of hepatic involvement, additional MRI of the liver seems to be beneficial for optimal treatment management.

References

[1] Oberg K, Castellano D. Current knowledge on diagnosis and staging of neuroendocrine tumors. Cancer Metastasis Rev 2011; 30(Suppl 1): 3–7. doi:10.1007/s10555-011-9292-1. PMid:21311954.

[2] Kaltsas GA, Papadogias D, Makras P, Grossman AB. Treatment of advanced neuroendocrine tumours with radiolabelled somatostatin analogues. Endocr Relat Cancer 2005; 12: 683–699. doi:10.1677/erc.1.01116. PMid:16322317.

[3] Yao JC, Hassan M, Phan A, et al. One hundred years after "carcinoid": epidemiology of and prognostic factors for neuroendocrine tumors in 35,825 cases in the United States. J Clin Oncol 2008; 26: 3063–3072. doi:10.1200/JCO.2007.15.4377. PMid:18565894.

[4] Oberg KE. Gastrointestinal neuroendocrine tumors. Ann Oncol 2010; 21(Suppl 7): vii72–vii80. doi:10.1093/annonc/mdq290. PMid:20943646.

[5] Koopmans KP, Neels ON, Kema IP, et al. Molecular imaging in neuroendocrine tumors: molecular uptake mechanisms and clinical results. Crit Rev Oncol Hematol 2009; 71: 199–213. doi:10.1016/j.critrevonc.2009.02.009. PMid:19362010.

[6] Kloppel G. Classification and pathology of gastroenteropancreatic neuroendocrine neoplasms. Endocr Relat Cancer 2011; 18(Suppl 1): S1–16. doi:10.1530/ERC-11-0013. PMid:22005112.

[7] Nisa L, Savelli G, Giubbini R. Yttrium-90 DOTATOC therapy in GEP-NET and other SST2 expressing tumors: a selected review. Ann Nucl Med 2011; 25: 75–85. doi:10.1007/s12149-010-0444-0. PMid:21107762.

[8] Reubi JC. Peptide receptor expression in GEP-NET. Virchows Arch 2007; 451(Suppl 1): S47–50. doi:10.1007/s00428-007-0443-2. PMid:17684767.

[9] Buchmann I, Henze M, Engelbrecht S, et al. Comparison of ^{68}Ga-DOTATOC PET and ^{111}In-DTPAOC (Octreoscan) SPECT in patients with neuroendocrine tumours. Eur J Nucl Med Mol Imaging 2007; 34: 1617–1626. doi:10.1007/s00259-007-0450-1. PMid:17520251.

[10] Gabriel M, Decristoforo C, Kendler D, et al. ^{68}Ga-DOTA-Tyr3-octreotide PET in neuroendocrine tumors: comparison w somatostatin receptor scintigraphy and CT. J Nucl Med 2007; 48: 508–518. doi:10.2967/jnumed.106.035667. PMid:17401086.

[11] Kwekkeboom DJ, Kam BL, van Essen M, et al. Somatostatin-receptor-based imaging and therapy of gastroenteropancreatic neuroendocrine tumors. Endocr Relat Cancer 2010; 17: R53–73. doi:10.1677/ERC-09-0078. PMid:19995807.

[12] Frilling A, Sotiropoulos GC, Radtke A, et al. The impact of ^{68}Ga-DOTATOC positron emission tomography/computed tomography on the multimodal management of patients with

neuroendocrine tumors. Ann Surg 2010; 252: 850–856. doi:10.1097/SLA.0b013e3181fd37e8. PMid:21037441.

[13] Ruf J, Heuck F, Schiefer J, et al. Impact of multiphase ^{68}Ga-DOTATOC-PET/CT on therapy management in patients with neuroendocrine tumors. Neuroendocrinology 2010; 91: 101–109. doi:10.1159/000265561. PMid:19996582.

[14] Schaefer JF, Schlemmer HP. Total-body MR-imaging in oncology. Eur Radiol 2006; 16: 2000–2015. doi:10.1007/s00330-006-0199-0. PMid:16622688.

[15] Lauenstein TC, Goehde SC, Herborn CU, et al. Whole-body MR imaging: evaluation of patients for metastases. Radiology 2004; 233: 139–148. doi:10.1148/radiol.2331030777. PMid:15317952.

[16] Muller-Horvat C, Radny P, Eigentler TK, et al. Prospective comparison of the impact on treatment decisions of whole-body magnetic resonance imaging and computed tomography in patients with metastatic malignant melanoma. Eur J Cancer 2006; 42: 342–350. doi:10.1016/j.ejca.2005.10.008. PMid:16364631.

[17] Pfannenberg C, Aschoff P, Schanz S, et al. Prospective comparison of ^{18}F-fluorodeoxyglucose positron emission tomography/computed tomography and whole-body magnetic resonance imaging in staging of advanced malignant melanoma. Eur J Cancer 2007; 43: 557–564. doi:10.1016/j.ejca.2006.11.014. PMid:17224266.

[18] Seemann MD, Meisetschlaeger G, Gaa J, Rummeny EJ. Assessment of the extent of metastases of gastrointestinal carcinoid tumors using whole-body PET, CT, MRI, PET/CT and PET/MRI. Eur J Med Res 2006; 11: 58–65. PMid:16504962.

[19] Scarsbrook AF, Ganeshan A, Statham J, et al. Anatomic and functional imaging of metastatic carcinoid tumors. Radiographics 2007; 27: 455–477. doi:10.1148/rg.272065058. PMid:17374863.

[20] Putzer D, Gabriel M, Henninger B, et al. Bone metastases in patients with neuroendocrine tumor: ^{68}Ga-DOTA-Tyr3-octreotide PET in comparison to CT and bone scintigraphy. J Nucl Med 2009; 50: 1214–1221. doi:10.2967/jnumed.108.060236. PMid:19617343.

[21] Prasad V, Baum RP. Biodistribution of the Ga-68 labeled somatostatin analogue DOTA-NOC in patients with neuroendocrine tumors: characterization of uptake in normal organs and tumor lesions. Q J Nucl Med Mol Imaging 2010; 54: 61–67. PMid:20168287.

[22] Virgolini I, Ambrosini V, Bomanji JB, et al. Procedure guidelines for PET/CT tumour imaging with ^{68}Ga-DOTA-conjugated peptides: ^{68}Ga-DOTA-TOC, ^{68}Ga-DOTA-NOC, ^{68}Ga-DOTA-TATE. Eur J Nucl Med Mol Imaging 2010; 37: 2004–2010. doi:10.1007/s00259-010-1512-3. PMid:20596866.

[23] Krausz Y, Rubinstein R, Appelbaum L, et al. Ga-68 DOTA-NOC uptake in the pancreas: pathological and physiological patterns. Clin Nucl Med 2012; 37: 57–62. doi:10.1097/RLU.0b013e3182393404. PMid:22157030.

[24] Kos-Kudla B, O'Toole D, Falconi M, et al. ENETS consensus guidelines for the management of bone and lung metastases from neuroendocrine tumors. Neuroendocrinology 2010; 91: 341–350. doi:10.1159/000287255. PMid:20484875.

[25] Steinmuller T, Kianmanesh R, Falconi M, et al. Consensus guidelines for the management of patients with liver metastases from digestive (neuro)endocrine tumors: foregut, midgut, hindgut, and

[26] Rodrigues M, Gabriel M, Heute D, et al. Concordance between results of somatostatin receptor scintigraphy with ^{111}In-DOTA-DPhe 1-Tyr 3-octreotide and chromogranin A assay in patients with neuroendocrine tumours. Eur J Nucl Med Mol Imaging 2008; 35: 1796–1802. doi:10.1007/s00259-008-0794-1. PMid:18425512.

[27] Hofland LJ, Lamberts SW. The pathophysiological consequences of somatostatin receptor internalization and resistance. Endocr Rev 2003; 24: 28–47. doi:10.1210/er.2000-0001. PMid:12588807.

[28] Ambrosini V, Campana D, Bodei L, et al. ^{68}Ga-DOTANOC PET/CT clinical impact in patients with neuroendocrine tumors. J Nucl Med 2010; 51: 669–673. doi:10.2967/jnumed.109.071712. PMid:20395323.

[29] Poeppel TD, Binse I, Petersenn S, et al. ^{68}Ga-DOTATOC versus ^{68}Ga-DOTATATE PET/CT in functional imaging of neuroendocrine tumors. J Nucl Med 2011; 52: 1864–1870. doi:10.2967/jnumed.111.091165. PMid:22072704.

[30] Adams S, Baum R, Rink T, et al. Limited value of fluorine-18 fluorodeoxyglucose positron emission tomography for the imaging of neuroendocrine tumours. Eur J Nucl Med 1998; 25: 79–83. doi:10.1007/s002590050197. PMid:9396878.

[31] Kayani I, Bomanji JB, Groves A, et al. Functional imaging of neuroendocrine tumors with combined PET/CT using ^{68}Ga-DOTATATE (DOTA-DPhe1,Tyr3-octreotate) and ^{18}F-FDG. Cancer 2008; 112: 2447–2455. doi:10.1002/cncr.23469. PMid:18383518.

[32] Ezziddin S, Lohmar J, Yong-Hing CJ, et al. Does the pretherapeutic tumor SUV in ^{68}Ga DOTATOC PET predict the absorbed dose of ^{177}Lu octreotate? Clin Nucl Med 2012; 37: e141–147. doi:10.1097/RLU.0b013e31823926e5. PMid:22614212.

[33] Miederer M, Seidl S, Buck A, et al. Correlation of immunohistopathological expression of somatostatin receptor 2 with standardised uptake values in ^{68}Ga-DOTATOC PET/CT. Eur J Nucl Med Mol Imaging 2009; 36: 48–52. doi:10.1007/s00259-008-0944-5. PMid:18807033.

[34] Koh DM, Collins DJ. Diffusion-weighted MRI in the body: applications and challenges in oncology. AJR Am J Roentgenol 2007; 188: 1622–1635. doi:10.2214/AJR.06.1403. PMid:17515386.

[35] Schwenzer NF, Schmidt H, Claussen CD. Whole-body MR/PET: applications in abdominal imaging. Abdom Imaging 2012; 37: 20–28. doi:10.1007/s00261-011-9809-7. PMid:22002195.

[36] Dorfman RE, Alpern MB, Gross BH, Sandler MA. Upper abdominal lymph nodes: criteria for normal size determined with CT. Radiology 1991; 180: 319–322. PMid:2068292.

[37] Glazer GM, Gross BH, Quint LE, et al. Normal mediastinal lymph nodes: number and size according to American Thoracic Society mapping. AJR Am J Roentgenol 1985; 144: 261–265. PMid:3871268.

[38] Sundin A, Vullierme MP, Kaltsas G, Plockinger U. ENETS Consensus Guidelines for the Standards of Care in Neuroendocrine Tumors: radiological examinations. Neuroendocrinology 2009; 90: 167–183. doi:10.1159/000184855. PMid:19077417.